

Honors Thesis

ELUCIDATING THE ROLE OF AGING IN PROTEIN MISFOLDING
AND AMYLOID CASCADE IN TRANSTHYRETIN AMYLOIDOSIS

by
Chad D. Hyer

Submitted to Brigham Young University in partial fulfillment
of graduation requirements for University Honors

Department of Chemistry and Biochemistry
Brigham Young University
December 2024

Advisor: Dr. John C. Price

Faculty Reader: Dr. Mark K. Transtrum

Honors Coordinator: Dr. Walter Paxton

ABSTRACT

ELUCIDATING THE ROLE OF AGING IN PROTEIN MISFOLDING AND THE AMYLOID CASCADE IN TRANSTHYRETIN AMYLOIDOSIS

Chad D. Hyer

Department of Microbiology and Molecular Biology
Bachelor of Science

Transthyretin Amyloidosis (ATTR) is a disease characterized by the misfolding and aggregation of a thyroid hormone transporter protein, transthyretin (TTR). Misfolding and aggregation of TTR is strongly correlated with aging and amyloidogenic mutations in TTR, but the pathogenesis of ATTR remains largely unknown. As a result, many ATTR patients remain undiagnosed and untreated until irreversible damage has occurred and until treatment methods become less effective. Traditional approaches to studying ATTR either do not approach TTR misfolding from a structural perspective or rely on methods that do not accurately probe changes in TTR structure under physiological conditions. As a result, little is known about how or why aging promotes TTR misfolding or the amyloid cascade.

This study investigates the role of aging in the pathogenesis of ATTR using the Iodine Protein Stability Assay (IPSA) on blood serum samples from a cohort of one hundred individuals aged 18-85 and overcomes limitations in previous studies by approaching TTR misfolding from a structural perspective, on a proteomic scale, and under physiological conditions in human subjects. Here we report on our preliminary findings in twenty subjects. Our findings suggest that aging increases proteolytic activity by reducing the effectiveness of serine protease inhibitors (SPIs) which then encourages TTR cleavage and misfolding, triggering the amyloid cascade. We also identify an unexpected axis of instability in TTR with aging that challenges existing models of TTR tetramer collapse. Additionally, we examine the role of protein folding stability (PFS) on protein turnover rates (TR) and amyloid clearance in six individuals and propose a model explaining the role of aging and protein stability in amyloid deposition and clearance.

Our study represents to our knowledge the first proteomic census of PFS in serum across age cohorts, and our preliminary findings shed light on the role of aging in the pathogenesis of ATTR and suggest a model explaining how protein misfolding and aggregation is promoted by age. Our findings showcase the strengths of IPSA for studying PFS across the proteome, particularly in the context of aging and amyloid diseases. We propose that quantifying PFS could serve as a diagnostic tool for proteome health and disease risk, and our approach introduces a new dimension and crucial perspective to studying the pathogenesis and pathophysiology of disease.

Keywords: transthyretin amyloidosis, aging, protein folding stability, protein misfolding, protein homeostasis, IPSA, turnover rate, structural proteomics, mass spectrometry

ACKNOWLEDGEMENTS

I would like to acknowledge my advisor Dr. JC Price. His willingness to take me into his lab and allow me to perform meaningful research under his supervision has completely changed my undergraduate experience and has given me opportunities to grow as a researcher and scientist. He didn't just have me clean glass. He gave me opportunities to meaningfully contribute to and be acknowledged for research and allowed me to help design and take on this study. His support, along with funding from the Department of Chemistry and Biochemistry at BYU, the NIH, and the Fritz B Burns Foundation, has made pursuing my research dreams possible. I also acknowledge the members of my committee for their assistance in the process of preparing my thesis. Special thanks to Dr. Transtrum for providing guidance in the analysis process and to Dr. Paxton for helping me navigate the honors thesis process.

I would also like to acknowledge other mentors, supporters, and contributors who have helped me through the process of preparing my thesis. Special thanks to Dr. Lavender Lin for taking me under her wing when I first entered the lab and for teaching me to be the researcher I am today. I also cannot fail to recognize her dedication and friendship to me. I will never forget her constant willingness to step up to the bat for me and to support me in all aspects of my life. Special thanks to my parents, Maren and David Hyer, for their constant support and willingness to listen to me throughout all the blood, sweat, and tears that went into making this study a reality. Special thanks as well to the other undergraduates and collaborators, Elli Vickers, Joshua Brown, and Dr. Leena Patil, who have helped make this study possible. Preparing all these samples by myself would have required another several years of work, and I appreciate the effort they put into helping make my thesis a possible undertaking as an undergraduate.

TABLE OF CONTENTS

Title.....	i
Abstract.....	ii
Acknowledgements.....	iii
Table of Contents.....	iv
List of Tables and Figures.....	v
I. Introduction.....	1
II. Methods.....	6
III. Results.....	14
IV. Discussion.....	26
V. Conclusions.....	31
References.....	34

LIST OF TABLES AND FIGURES

Figure 1.....	3
Figure 2.....	4
Figure 3.....	14
Figure 4.....	16
Figure 5.....	17
Table 1.....	18
Figure 6.....	19
Figure 7.....	21
Figure 8.....	22
Table 2.....	22
Figure 9.....	24
Figure 10.....	27
Figure 11.....	28
Equation 1.....	29
Equation 2.....	29
Figure 12.....	30

Introduction

All forms of life are composed of proteins that perform most biological functions. Proteins are macromolecules composed of chains of amino acids that fold into complex structures that determine their functions. Protein folding is essential to the proper function of proteins and to maintaining homeostasis, and misfolding can contribute to the aggregation of protein amyloids and disruption of proteostasis.¹

As humans age, levels of misfolded proteins increase.² Protein misfolding with age has been extensively studied and has been attributed to a variety of causes such as oxidative damage, chaperone dysfunction, proteolysis dysregulation, and other factors,³ but much of protein misfolding and aggregation is still not understood.⁴ This increased propensity of misfolding with age has been implicated in the development of many diseases such as Alzheimer's, Parkinson's, type 2 diabetes, and transthyretin amyloidosis.¹

One such example of misfolding disease, transthyretin amyloidosis (ATTR) is characterized by the misfolding and aggregation of a thyroid hormone transporter protein, transthyretin (TTR, Uniprot Accession: P02766 | TTHY_HUMAN). Previously assumed to be a rare disease, diagnoses of ATTR are becoming more common due to increased recognition of its pathology, but diagnosis is still difficult and can be invasive, leading to later diagnosis, irreversible damage, and decreased treatment effectiveness.⁵ ATTR dramatically lowers quality of life and is typically fatal, and early diagnosis is essential for effective treatment.⁶ Hence, improvements in diagnostic methods and our understanding of ATTR are essential to treating this disease.

The mechanisms and pathogenesis of ATTR, however, are not well understood. Aging and a variety of amyloidogenic mutations have been linked to increased risk of developing ATTR, but much about the mechanisms of these risk factors remains unknown.⁷ Currently, there are two prevailing models for the proposed mechanism of ATTR pathogenesis, the kinetic instability model and the proteolytic cleavage model (Figure 1). An important note to make for the discussion throughout this paper is that all references to residue numbers will be done based on canonical Uniprot FASTA residue numbers. Within much ATTR literature, the first twenty amino acids are removed from the numbering scheme as they are cleaved after translation (Ex: Uniprot K68 → Literature K48).

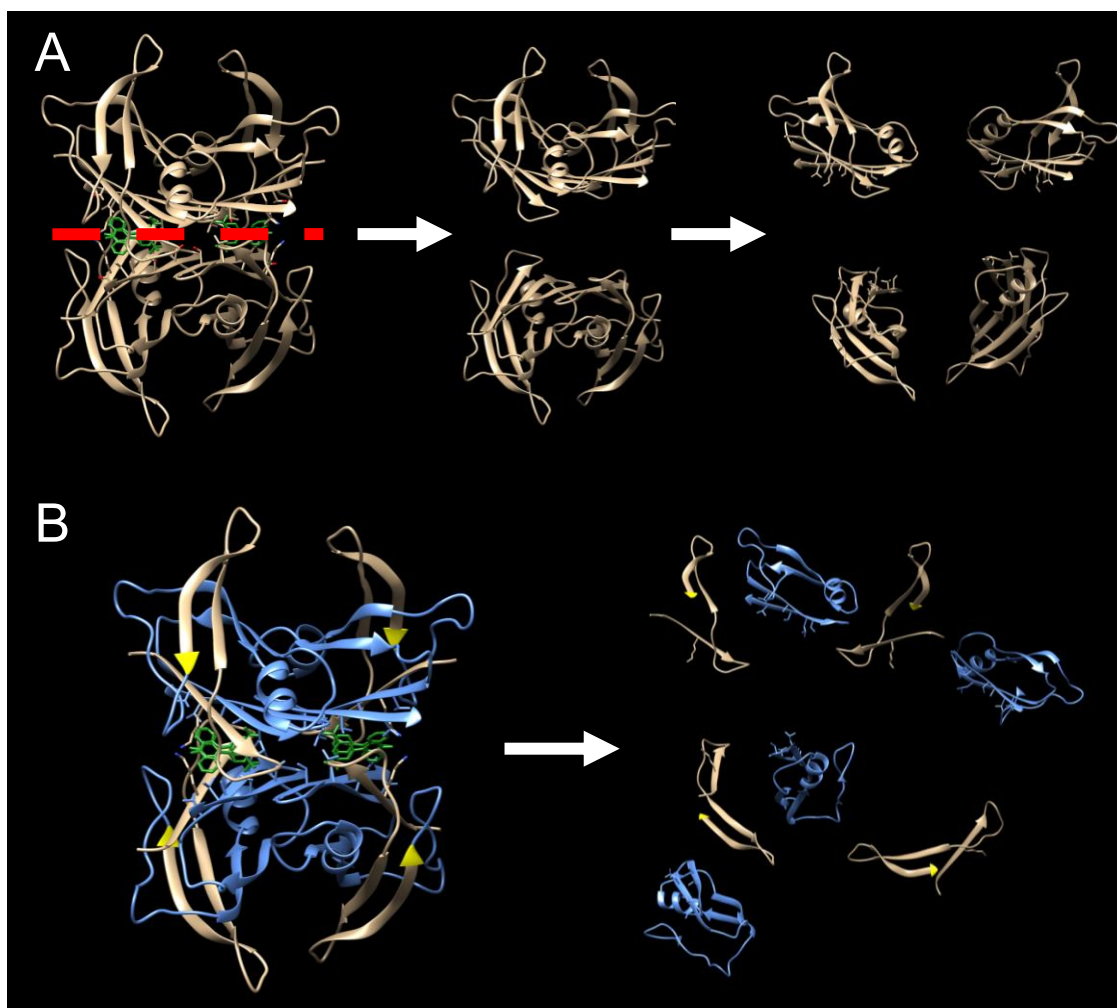


Figure 1: ATTR Models. (A) Kinetic Instability Model: TTR tetramers dissociate along the axis of the homodimer interface (red) into dimers that can further dissociate into monomers that are prone to misfolding and aggregation.⁸ (B) Proteolytic Cleavage Model: TTR tetramers are cleaved at K68 (yellow) by serum proteases encouraging dissociation into the 69-147 fragment (blue) and 1-68 fragment (tan) that are prone to misfolding and aggregation.⁹ TTR structures were obtained from Protein Data Bank (PDB) entry 1BM7.¹⁰

Both models are reported in the literature and appear to be implicated and supported by different amyloidogenic mutations (Figure 2). For example, the kinetic instability model is supported by decreases in tetramer stability associated with mutations near the homodimer axis such as V142I.¹¹ The proteolytic cleavage model, on the other hand, is supported by mutations near the K69 cleavage site such as V50M causing

increased susceptibility to proteolysis.¹² Both models are plausible and have literature support, but it is yet to be known which model plays a greater role in the pathogenesis of ATTR and what role aging plays in these mechanisms.

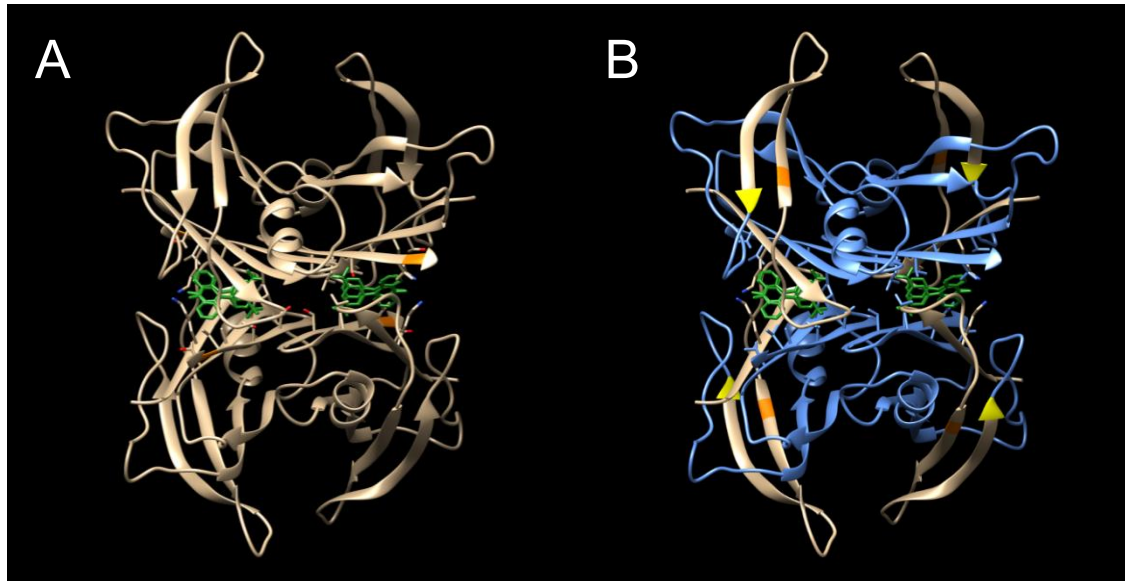


Figure 2: Amyloidogenic Mutations in ATTR. (A) V50M (orange) is located along the homodimer interface and putatively increases rates of tetramer dissociation. (B) V142I (orange) is near the K68 cleavage site (yellow) and putatively increases TTR's susceptibility to proteolysis.

Existing research on these models has struggled to provide conclusive results for either model within clinical settings due to various limitations in their methodologies. Traditionally, most studies have utilized methodologies that examine abundances of biomarkers rather than probing structural differences.¹³ While tracking biomarker concentrations has provided great insight into many diseases, it fails to capture the biophysical roots of protein-misfolding diseases. Methodologies from studies that do approach amyloid diseases from a structural perspective, on the other hand, have relied on subjecting proteins to nonnative conditions that do not accurately represent physiological conditions and are usually unable to probe changes in protein structure with

adequate throughput to understand the impacts of structural changes on a proteomic scale.¹³

Recent advances in the field of structural proteomics such as the Iodine Protein Stability Assay (IPSA), remedy flaws in existing methodologies by allowing for the quantification of protein folding stability (PFS) on a proteomic scale, with residue-specific resolution, and under physiological conditions.¹³ Hence, applying IPSA to the study of ATTR can potentially elucidate the role of aging and structural differences in TTR misfolding and the amyloid cascade and can potentially provide physiologically significant insight into the pathogenesis of ATTR, allowing for the development of better, clinically-relevant diagnostic and treatment methods.

In this study, we demonstrate the use of IPSA on subset of serum samples from a cohort of one hundred fifty individuals aged 18-85. We investigate the role of aging in the pathogenesis of ATTR by quantifying and comparing the residue-specific PFS for the top proteins in the serum proteome, including TTR, across age cohorts. Reported are our preliminary findings in twenty subjects. Additionally, we examine the role of PFS on protein turnover rates (TR) in six individuals to elucidate the role of protein stability in amyloid deposition.

Our study represents to our knowledge the first proteomic census of PFS in serum across age cohorts and sheds light on the role of aging in the pathogenesis of ATTR and suggests a model by which protein misfolding and aggregation is promoted by age. Our findings showcase the strengths of IPSA for studying PFS across the proteome, particularly in the context of aging and amyloid diseases. We propose that quantifying PFS could serve as a diagnostic tool for proteome health and disease risk, and our

approach introduces a new dimension and crucial perspective to studying the pathogenesis and pathophysiology of amyloid diseases.

Methods

Sample Collection and Selection

Blood serum samples were collected at Brigham Young University (BYU IRB# 2022-200) from 150 subjects aged 18-85. Study participants were recruited voluntarily and randomly to reduce potential bias in the results. We acknowledge, however, that, due to constraints in resources for collection, most samples were collected from individuals of European descent who live or have lived near Brigham Young University. In future work, we intend to include more diversity in sampling.

Using a questionnaire, we anonymously collected information on age, sex, BMI, family history of amyloidosis, and lifestyle factors such as alcohol consumption, tobacco use, and prescription drug use. From the 150 individuals sampled, we selected 10 males and 10 females from age groups 18-29, 30-39, 40-49, 50-59, 60+ for a total of 100 participants. The selection was mostly random, but attention was given to history of prescription drug use with increased weighting towards individuals taking fewer prescription drugs to limit the bias of drug binding effects in our analysis of age-dependent differences in PFS.

Serum samples for our protein turnover (TR) comparison were kindly provided by Dr. Brad Naylor from previously published work.¹⁴ All serum sample protein concentrations were determined using a bicinchoninic acid assay (BCA) (ThermoFisher #23225) and were diluted to 10 mg/mL in 50 mM Tris (pH 7.4) and aliquoted into

volumes that had sufficient protein for use in a single experiment to avoid impacts of freeze/thaw cycles on protein structure. All samples were then stored at -80 °C until used.

Exome Sequencing and Bioinformatic Analysis

Whole blood samples of the 100 individuals selected were sent to GENEWIZ from Azenta Life Sciences for whole-exome sequencing. DNA quantification was performed using a Qubit 2.0 Fluorometer (ThermoFisher Scientific). Twist Human Core Exome library preparation was then performed. DNA was fragmented using a Covaris S220. Fragmented DNA was cleaned up, end repaired, and adenylated at the 3' ends. Illumina Y-shaped adapters were then ligated onto the DNA fragments, and the adapter-ligated DNA fragments were amplified using limited cycle PCR and quantified using a Qubit 2.0 Fluorometer. Adapter-ligated DNA fragments were then hybridized with biotinylated baits, and hybrid DNAs were captured using streptavidin-coated beads and washed.

Captured DNAs were then amplified and indexed with Illumina indexing primers. Post-captured DNA libraries were validated using an Agilent TapeStation and quantified using a Qubit 2.0 Fluorometer and Real-Time PCR (KAPA Biosystems). Next-generation sequencing was performed using an Illumina Nova instrument. NovaSeq Control software was used for image analysis and base calling. Raw sequence data was then converted to fastq files and de-multiplexed using Illumina bclfastq 2.17. Somatic SNVs and small indels were then called using Sentieon 202112.01 (TNseq algorithm), and generated variant call format (VCF) files were normalized using version 1.13 of the bcftools software package.¹⁵ Overlapping transcripts were identified for each variant and variant effects were predicted using Ensembl VEP 104.

Using the VCF files generated by GENEWIZ, we generated custom protein FASTAs for each subject using a modified form of SnpEffect produced by the Lloyd Smith Group at the University of Wisconsin as part of the Spritz software package.¹⁶ Generated variant sequences for each protein were combined within each subject to create one amino acid sequence per protein and were added to the canonical *Homo sapiens* FASTA downloaded from UniprotKB (downloaded in March 2023), replacing entries so as to only have one sequence per protein.

Sample Blocking and Randomization

To reduce the impacts of time-dependent instrument drift and imbalanced noise due to randomization, we block randomized serum samples from our 100 subjects according to methods specified by Burger, et al.¹⁷ Samples were blocked into groups of four subjects based on sex and age with each sample batch containing an individual aged 18-34, 35-49, 49-64, and 65+, all of the same sex. Individuals were added to batches at random to remove any bias in blocking.

Iodine Protein Stability Assay (IPSA) and Quantitative Proteomics

Following the protocol published by Lin, et al.¹³ with some modifications, we performed IPSA on each batch of four subjects and the six turnover rate (TR) samples. We also performed a standard proteomics serum digest for quantitative proteomics analysis to calculate the relative abundances of proteins in the serum of each subject.

For IPSA, 10 aliquots of 20 μ L of serum (10 mg/mL) from each subject were loaded into polymerase chain reaction (PCR) strips. Each aliquot was unfolded using a gradient of guanidinium chloride (GdmCl in 50 mM Tris, pH 8.5) concentrations (0, 0.75, 1.5, 2.25, 3, 3.75, 4.5, 5.25, 6, and 6.2 M). 27.6 μ L of GdmCl were added to each sample

according to its assigned point in the gradient, and each aliquot was incubated at 37 °C for 30 minutes. 2 µL of iodine (150 mM I₂ in 600 mM KI) was then added to each aliquot to label surface-exposed amino acids, and samples were incubated at 37 °C for 15 minutes. The labeling reaction was then quenched using 50 µL of 150 mM imidazole, and samples were incubated at room temperature for 5 minutes.

After IPISA, 100 µL of 6M GdmCl was then added to each aliquot to fully denature each sample. An additional 20 µL serum (10 mg/mL) aliquot was created at this time for quantitative proteomics comparisons between subjects. Only the aliquot slated for quantitative proteomics analysis was then reduced and alkylated using 9 µL of 500 mM tris(2-carboxyethyl)phosphine hydrochloride (TCEP) and 36 µL of 500 mM 2-chloroacetamide (CAA), incubated at 100 °C for 5 minutes, and sonicated in a water bath for 5 minutes.

All samples were then transferred to 30 kDa spin filters. Samples were then washed twice using 200 µL 25 mM ammonium bicarbonate (ABC) in 20% acetonitrile (ACN) with 30 minutes of centrifuging at 14,000 x g for each wash. Samples were then resuspended in 300 µL of ABC wash buffer and 4 µL of liquid chromatography-mass spectrometry (LCMS)-grade trypsin protease (1 µg/ µL) (Pierce, Cat# 90058) and were incubated at 37 °C with shaking overnight for protein digestion. Digested peptides were then collected by spinning at 14,000 x g for 30 minutes. A second wash using 100 µL ABC wash buffer was performed at the same speed. The filtrate was then transferred to mass spec (MS) vials and dried in a SpeedVac concentrator (SAVANT SPD131DDA) and were then resuspended in 0.1% formic acid in 3% acetonitrile. Samples were then stored at -20 °C before MS acquisition.

LCMS/MS Acquisition

Each batch was submitted to the BYU Mass Spectrometry Core Facility for mass spectrometric (MS) acquisition. Within each batch, sample set run order was randomized, and run order of each of the 10 aliquots within each sample set was randomized.

LCMS/MS acquisition was performed according to the parameters specified in the “Agilent 6560-LFQ Method” section of the work of Lin, et al.¹³

Protein Identification and Quantification

Data files generated from MS analysis were analyzed to identify and quantify detected peptides and proteins using PEAKS 11 (Bioinformatics Solution Inc). PEAKS identification and quantification was performed using the settings and parameters specified in the “Identification and Quantification” section of the work of Lin, et al.¹³ Custom protein FASTAs described earlier were used as the database for the peptide identification in each subject’s sample. Label free quantification (LFQ) of proteins and peptides was performed using the LFQ module of PEAKS and associated LFQ files were exported for further analysis.

PFS Calculation

LFQ files from PEAKS analysis with relative abundances of detected proteins and peptides were analyzed using CHalf v4.2.1¹⁸ to calculate the PFS ($C_{1/2}$ values) of the labeled proteins within our first twenty subjects. CHalf settings included individual rep analysis, combined analysis, remove outlier analysis, four minimum points for calculation, a two standard error cutoff for outliers, label efficiency, and fitting efficiency with a 0-3.48 $C_{1/2}$ range cutoff, a 0.6 r^2 cutoff, and a 0.35 ratio to range confidence interval cutoff. Combined Label Sites files for each subject were then exported for later analysis.

PFS-Age Analysis

$C_{1/2}$ values for labeled residues within proteins were extracted from each of the Combined Label Sites files for each subject. Two forms of PFS analysis were performed. A residue-level analysis was performed by averaging $C_{1/2}$ values for residues with multiple measured $C_{1/2}$ values within each subject to produce a subject-specific protein-residue-number $C_{1/2}$ value. Residues with single measurements were also included in the

analysis. All residue-level measurements were then associated with the ages of the subjects. Each identified $C_{1/2}$ value that occurred at the same residue in the same protein of each subject was then compared using a Spearman rank correlation test to assess if a monotonic correlation existed between age and PFS at each site. Any site with fewer than five data points in between subjects was excluded from the analysis. Data points with a p-value less than 0.05 and a Spearman coefficient greater than 0.25 or less than -0.25 were considered significant and were separated for further analysis.

A protein-level analysis was also performed by averaging all $C_{1/2}$ values measured at any residue in a protein within each subject to produce a subject-specific protein $C_{1/2}$ value. All protein $C_{1/2}$ values were then associated with the ages of the subjects. Protein $C_{1/2}$ values of each subject were then compared using a Spearman rank correlation test to assess if a monotonic correlation existed between age and PFS within each protein. Any protein with fewer than five data points in between subjects was excluded from the analysis. Data points with a p-value less than 0.05 and a Spearman coefficient greater than 0.25 or less than -0.25 were considered significant and were separated for further analysis.

Combined PFS-Turnover Analysis

$C_{1/2}$ values for labeled residues within proteins were extracted from each of the Combined Label Sites files for each subject. Protein turnover rates (TR), the rates at which proteins are synthesized and degraded within the body, were previously calculated by Naylor, et al.¹⁴ Subject-specific protein $C_{1/2}$ values were calculated by averaging all $C_{1/2}$ values measured at any residue in a protein within each subject to produce a subject-specific protein $C_{1/2}$ value. Protein $C_{1/2}$ values were then paired with protein TRs and

compared using a Spearman rank correlation test to assess if a monotonic correlation existed between TR and PFS.

Results

PFS-Age Analysis

MS analysis of samples for our PFS-Age analysis within our subcohort of twenty individuals identified and quantified 3218 proteins and 9017 unique peptides. CHalf analysis calculated PFS in 300 proteins and calculated 1001 unique residue-specific $C_{1/2}$ values with an average labeling efficiency of 65.85% and an average fitting efficiency of 26.18%. Generally, quantifiable $C_{1/2}$ values were not consistently shared between subjects, so we limited analysis to data points shared by at least five subjects (Figure 3).

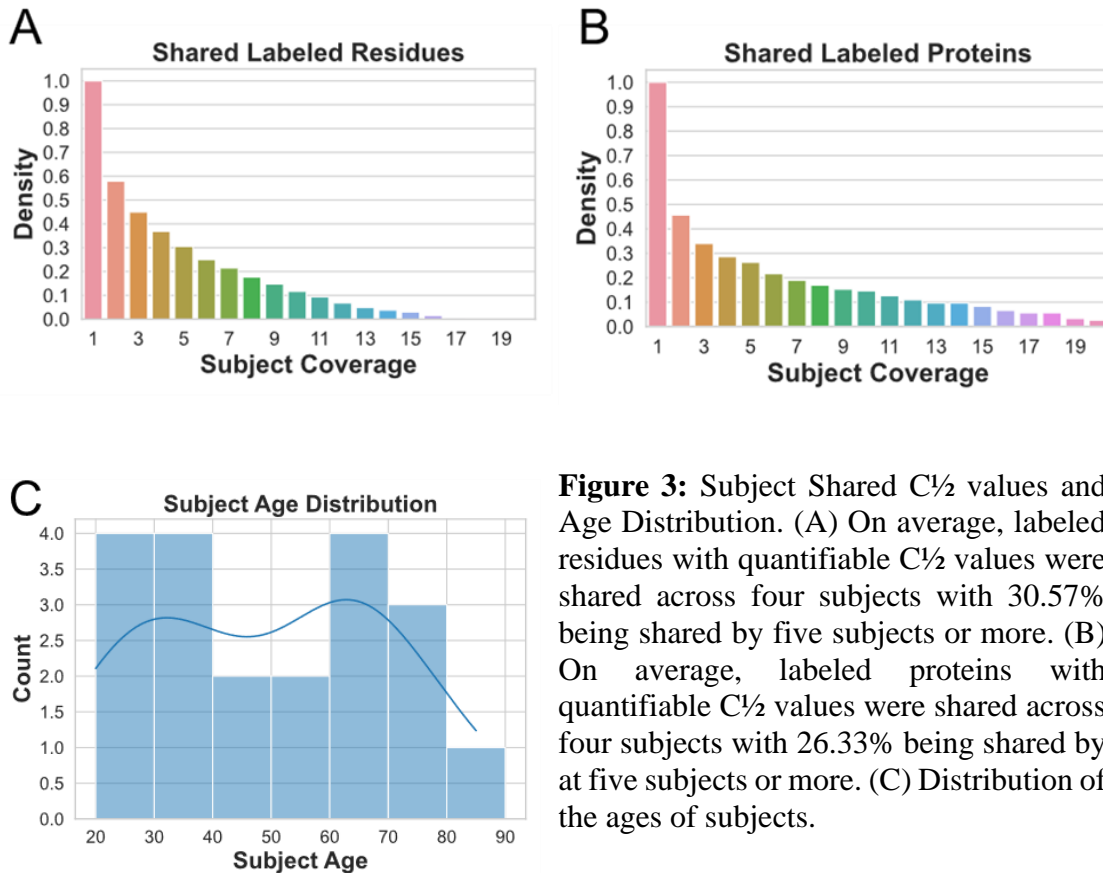


Figure 3: Subject Shared $C_{1/2}$ values and Age Distribution. (A) On average, labeled residues with quantifiable $C_{1/2}$ values were shared across four subjects with 30.57% being shared by five subjects or more. (B) On average, labeled proteins with quantifiable $C_{1/2}$ values were shared across four subjects with 26.33% being shared by at five subjects or more. (C) Distribution of the ages of subjects.

Examining the results of our Spearman correlation tests, we identified seven proteins significantly implicated with age (Figure 4A). We also identified twenty-one

labeled residues significantly implicated with age (Figure 4B). We also observed a general tendency towards decreased PFS with age on both a protein (Spearman=-0.09586, p=0.0009) and residue-specific (Spearman=-0.05043, p=0.0012) level. This tendency was more apparent in protein level analysis than residue level analysis, but this was to be expected as different portions of proteins have unique $C_{1/2}$ values and can experience changes in PFS independent of the whole protein.¹³

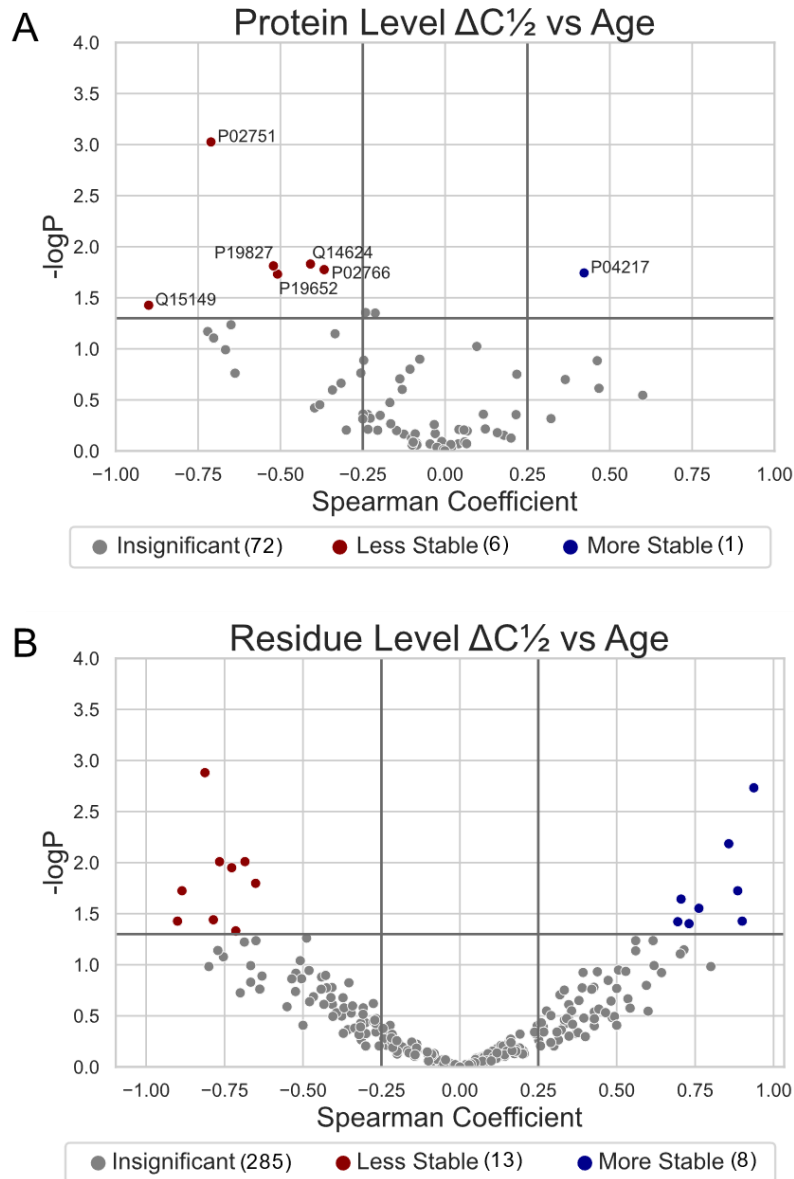


Figure 4: Volcano Plots of Impact of Age on PFS: (A) Six proteins are less stable (red) whereas one is more stable (blue) with age. (B) Thirteen labeled residues are less stable (red) whereas eight are more stable (blue) with age.

Examining the functions of proteins with significantly different PFS as well as proteins associated with labeled residues impacted by aging based on their Uniprot accessions, we identified six groupings of proteins with similar functions and compared how aging impacted PFS within each group (Figure 5). Proteins that compose each group can be found in Table 1.

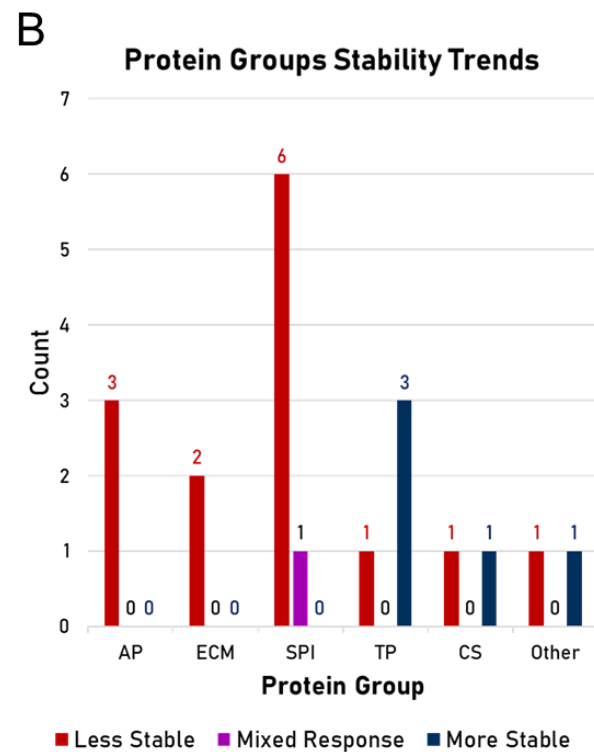
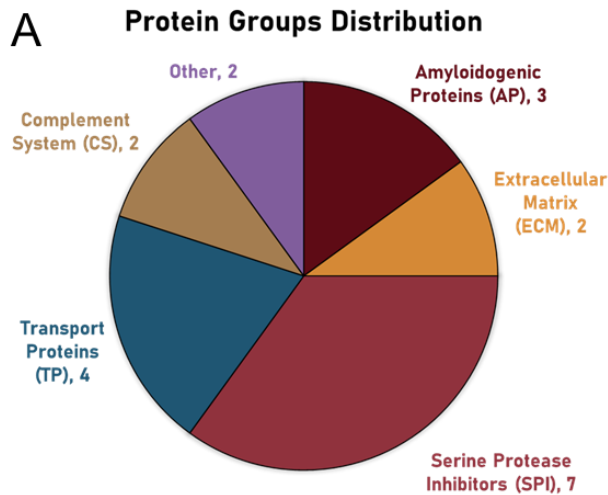


Figure 5: Proteins Grouped by Function.

(A) Proteins significantly impacted by age were grouped into six groups based on their function: amyloidogenic proteins (AP, n=3), extracellular matrix proteins (ECM, n=2), serine protease inhibitors (SPI, n=7), transport proteins (TP, n=4), complement system proteins (CS, n=2), and other proteins (n=2).

(B) Examining the trends within each protein group, APP, ECM, and SPI tended to be less stable with age (red) while TP tended to be more stable with age (blue). CS and other did not appear to exhibit a specific trend. Proteins in groups with mixed response (purple) experienced both increases and decreases in stability of labeled residues across different domains.

Stability trends of proteins within each group were examined within the context of ATTR. Future discussion will focus on AP, ECM, and SPI due to connections to ATTR pathology and mechanisms. We leave further discussion of other groups for future work as it is not within the scope of this paper.

AP	SPI	ECM	TP	CS	Other
P02766 TTHY	P01009 A1AT	Q15149 PLEC	P06727 APOA4	P08603 CFAH	P02765 FETUA
P01857 IGHG1	P01011 AACT	P02751 FINC	P02647 APOA1	P05155 IC1	P04217 A1BG
P0DOX5 IGG1	P19652 A1AG2		P04114 APOB		
	P19652 ITIH1		P02787 TRFE		
	P19823 ITIH2				
	Q14624 ITIH4				
	P01023 A2MG				

Table 1: Protein Groups Composition. Uniprot accessions of proteins that composed each protein group (defined in Figure 5A) as well as their stability trends. Decreased stability is in red, increased stability is in blue, and mixed response is in purple. Proteins were manually assigned to groups based on annotated functions in the Uniprot database.

Transthyretin

Examining proteins changed with age from the AP group, transthyretin (TTR, Uniprot: P02766 TTHY) experienced significant decreases in stability with age on both a protein and residue-specific level (Figure 6). Other implicated proteins from AP, IGHG1 and IGG1, were also significantly less stable with age. IGHG1 and IGG1, are associated with heavy chain amyloidosis (AH), a different amyloid disease, so further discussion will not include these proteins as they are out of the scope of this paper. TTR is the primary protein involved in ATTR, so this discussion will focus on changes in PFS observed in TTR. We do find it interesting to note, however, that proteins implicated in amyloid diseases exhibit a trend of decreased stability in the serum soluble fraction with age and intend to perform deeper analysis on AP implicated proteins in future work as we continue this study.

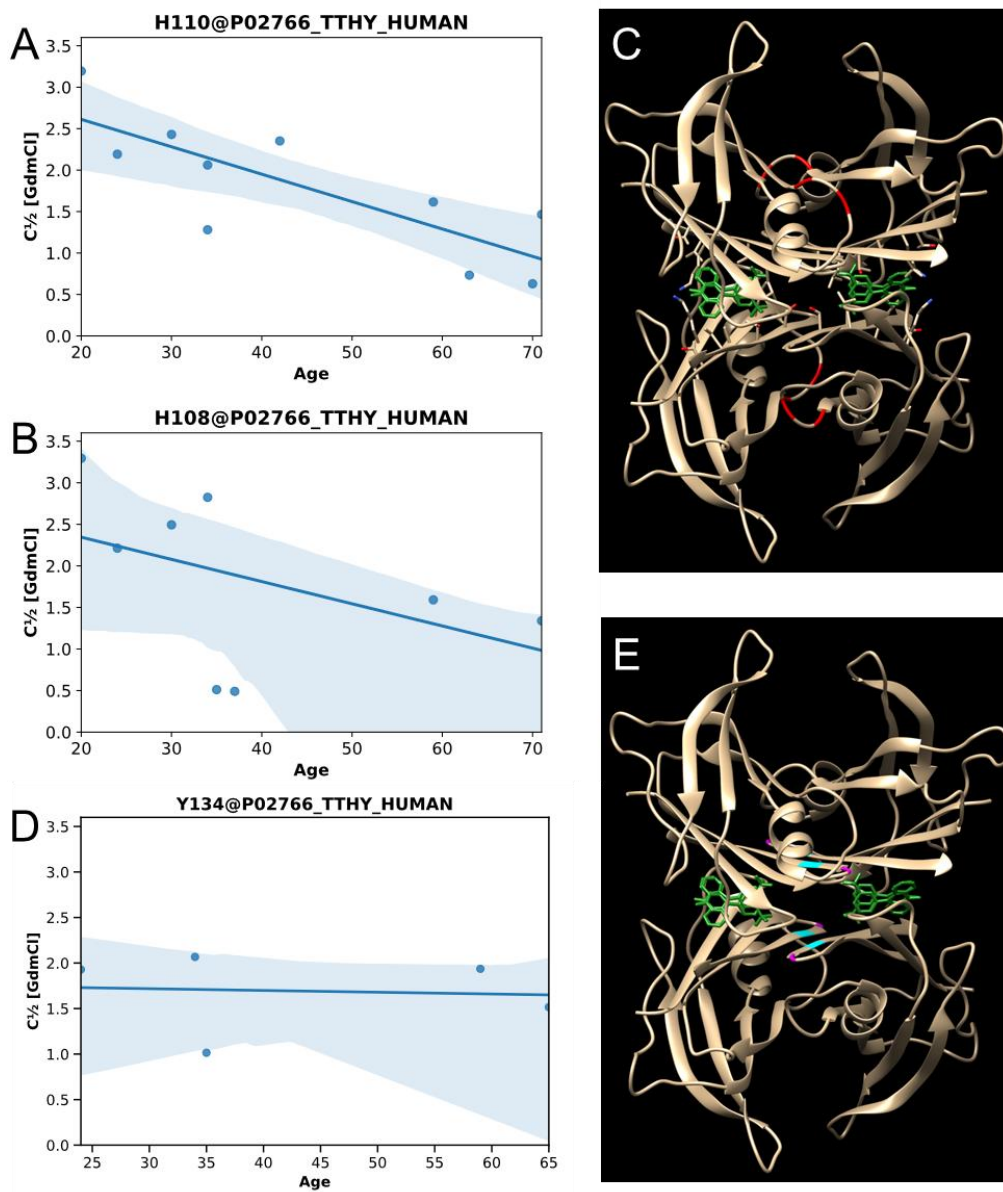
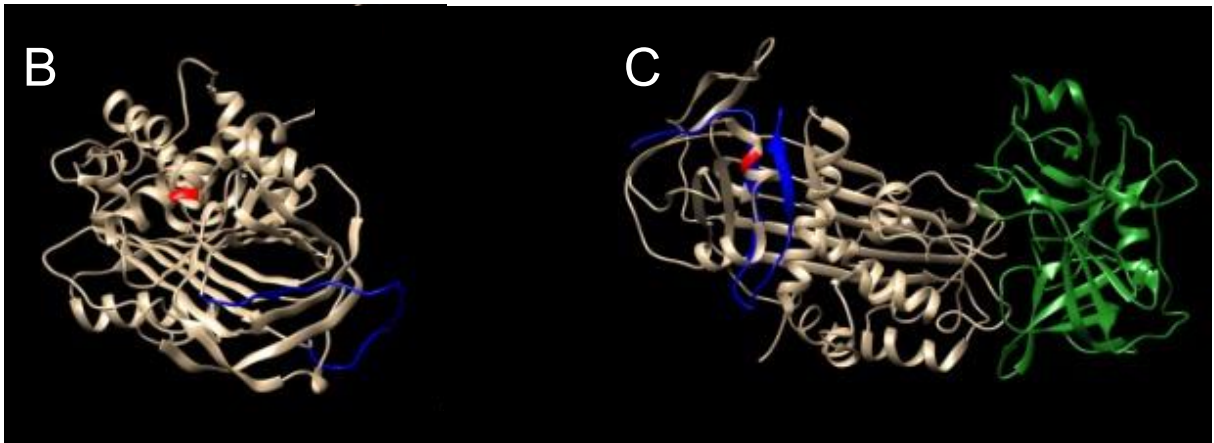
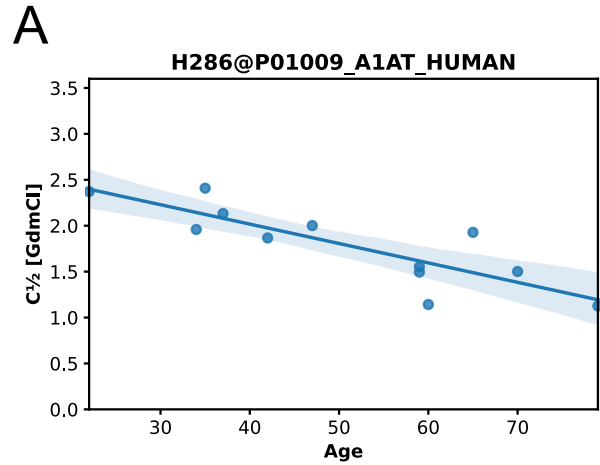


Figure 6: Impacts of Age on TTR PFS. (A) Residue H110 in TTR experiences significant decreases in stability with age with a Spearman coefficient of -0.766 ($p=0.00979$, $n=10$). (B) Residue H108 in TTR also experiences a significant decrease in stability with age with a Spearman coefficient of -0.714 ($p=0.04653$, $n=8$). (C) H108 and H110 (red) lie along the monomer interface within TTR dimers suggesting that age encourages tetramer instability along the dimer (vertical) axis. (D, E) Residue Y134 (pink) on the homodimer interface has no significant change in PFS with age with a Spearman coefficient of -0.3 ($p=0.62384$, $n=5$). Y136 (cyan), also at the homodimer interface, did not have enough points for a robust analysis but also had no change in stability with age, suggesting no change in stability along the homodimer (horizontal) axis. Hence, TTR dimers appear to experience decreased stability with age whereas homodimer stability appears to be unchanged.

Serine Protease Inhibitors

Proteases have previously been implicated in the pathogenesis of ATTR.⁹ Supporting these literature observations we also observe significant age-dependent changes in PFS of serine protease inhibitors (SPIs) in our data. Examining the impact of age on SPIs, we overwhelmingly observed significant decreases in PFS of various SPIs at both a protein and residue-specific level (Table 2). To interpret the residue-specific changes in PFS structurally, we used AlphaFold^{19, 20} and experimental protein structures which showed that residues with decreased stability were generally located in protease-binding sites of SPIs, within bait regions, or were residues that interacted with bait regions post-protease-SPI complex formation (Figures 7 and 8). Notably, SPI inhibitory efficiency is determined by the ability of the bait region to insert into middle-strand positions, post-protease-cleavage (Figure 7C).²¹ Decreases in PFS within these regions with age hence likely have functional significance.

Figure 7: Impact of Age on PFS in A1AT. (A) H286 exhibits decreased PFS with age with a Spearman coefficient of -0.8126 ($p=0.0013$, $n=12$). (B) In unbound A1AT, H286 (red) is surface exposed and far from the 368-392 bait region (blue) (AF-P01009), whereas (C) binding of elastase (green) to A1AT leads to the tucking of the cleaved bait region into the domain surrounding H286, decreasing H286 surface accessibility and increasing PFS.²² Decreased PFS with age suggests decreased A1AT binding efficiency with target proteases.



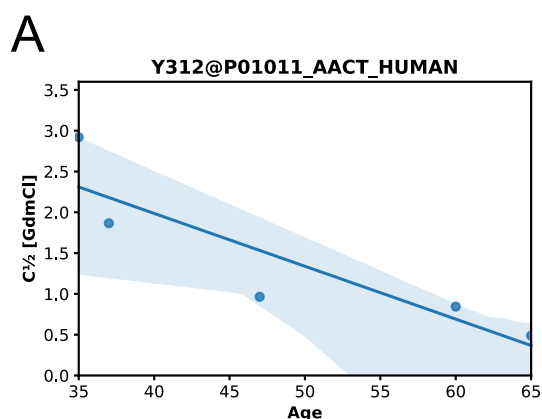
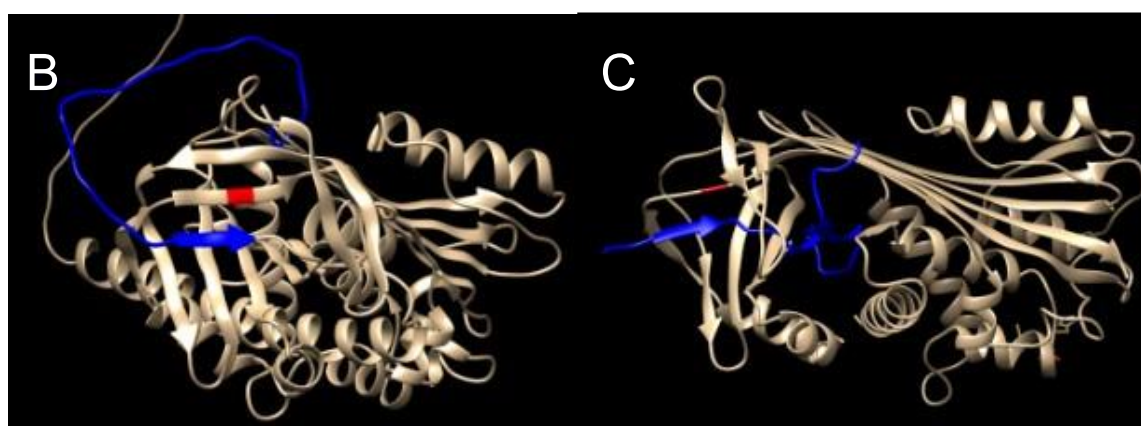


Figure 8: Impact of Age on PFS in AACT. (A) Y312 exhibits decreased PFS with age with a Spearman coefficient of -1 ($p=1.4 \times 10^{-24}$, $n=5$). (B) In unbound AACT, Y312 (red) is surface exposed and is part of a beta sheet interacting with the 369-394 bait region (blue) (AF-P01011), whereas (C) binding of a protease leads to the conversion of Y312 to a loop domain²³ interacting with a separate portion of the cleaved bait region and the formation of an ultra-stable AACT-protease complex.²⁴ Decreased PFS with age suggests decreased AACT binding to target proteases.



Accession	Location	Spearman	p-value	n	Δ PFS
Q14624 ITIH4	Protein level	-0.4088	0.0148	15	↓
P19827 ITIH1	Protein level	-0.5212	0.0154	12	↓
P19652 A1AG2	Protein level	-0.5087	0.0185	10	↓
P01011 AACT	Y312	-1	1.4×10^{-24}	5	↓
P01009 A1AT	H286	-0.8126	0.0013	12	↓
P19823 ITIH2	M85	-0.9	0.0374	5	↓
P01023 A2MG	Y138	-0.685	0.0098	12	↓
	Y708	0.937	0.0019	7	↑
	Y1104	0.9	0.0374	5	↑

Table 2: Impacts of Age on PFS of Serine Protease Inhibitors. Red text represents decreases in stability, blue text represents increases in stability, and purple text represents a mixed response. SPIs overwhelmingly experience decreases in PFS with age with only A2MG being the exception with a mixed response. Structural analysis did not provide a conclusive explanation for the mixed response in A2MG due to limitations in existing bound and unbound A2MG PDB structures, but we hypothesize that the mixed response is a result of differential protease binding with age and different domains in A2MG experiencing different conformational changes with protease binding.

Extracellular Matrix

We observed significant decreases in stability for two ECM proteins, fibronectin (Uniprot: P02751|FINC, Spearman=-0.7109, p=0.0009, n=5) and plectin (Uniprot: Q15149|PLEC, Spearman=-0.9, p=0.0374, n=5). ECM proteins are implicated in ATTR,²⁵ aging,²⁶ and serum protease activity,²⁷ so it is interesting that we observed significant decreases in ECM PFS. Consistent with literature findings, fibronectin stability decreases with age.²⁸ Instability and increased proteolytic cleavage of fibronectin is also associated with degeneration and other amyloid diseases such as Parkinson's and Alzheimer's.^{29, 30} Similarly, increased plectin cleavage and dysfunction is associated with age and sarcopenias that can contribute to muscular dystrophies that can occur with aging and ATTR.³¹⁻³⁴ Considering the role of proteolysis in ECM degradation, we posit that changes in ECM PFS can act as a proxy metric of proteolytic activity. Hence, we hypothesize that the observed decreases in PFS of ECM proteins with aging are a result of increased proteolytic activity due to decreased SPI binding efficiency.

PFS-TR Analysis

Comparing the PFS data obtained from performing IPISA on serum samples provided by Dr. Brad Naylor with published turnover rate (TR) data¹⁴ obtained from these same samples, we found a significant negative correlation between TR and PFS for blood proteins (Figure 9).

Turnover Rate vs Protein Folding Stability

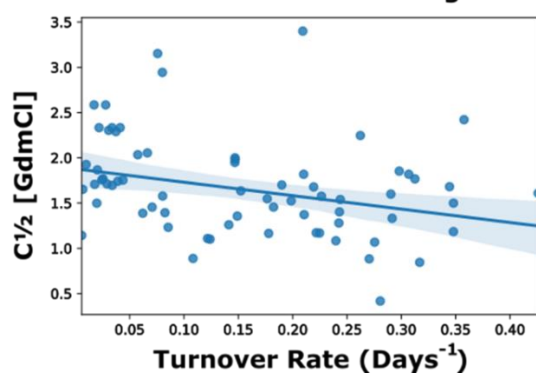


Figure 9: Turnover Rate vs Protein Folding Stability. PFS is negatively correlated with TR (Spearman=-0.35, $p=0.0034$). Using a robust linear regression, we find a relationship of $C_{1/2} = 1.877 - 1.483(TR)$ (intercept $p=1.84E-8$, slope $p=0.003$). This finding suggests that more stable proteins are either synthesized or degraded at a slower rate than less stable proteins.

Within the context of amyloid diseases, previous work has demonstrated that amyloids are thermodynamically more stable than native folding states and experience decreased degradation rates.^{35, 36} Most forms of protein degradation rely on the surface accessibility of targetable residues³⁷ or on ATP-mediated unfolding of proteins before degradation³⁸, we hypothesize that slower TR with increased PFS can most probably be attributed to decreased rates of degradation.

Previous work has also demonstrated that proteins with higher turnover rates tend to have increased propensity for aggregation and amyloid formation.³⁹ Decreased PFS has also been correlated with increased propensity for aggregation and amyloid formation.⁴⁰ Combining our finding of decreased TR and increased PFS reinforces the idea that amyloid accumulation could be primarily due to the misfolded protein resisting unfolding and proteolytic degradation. We hypothesize that PFS plays a major role in maintaining proteostasis by controlling both the propensity of a protein to form amyloids and the ability of the body to clear out amyloids using proteolytic maintenance mechanisms. This finding has not previously been demonstrated and challenges the prevailing assumption that PFS only plays a minor role in TR.⁴¹ Applying this finding within the context of ATTR, we observed a mean $C_{1/2}$ value of 1.307 M GdmCl and an

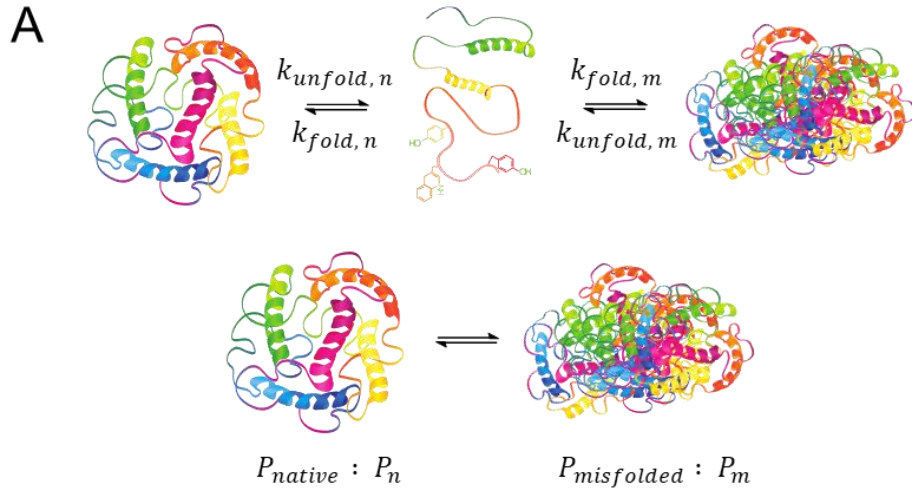
average TR of 0.2425 for healthy TTR. Extrapolating based on our experimental data and trendline, we expect a $C_{1/2}$ value of 1.699 M GdmCl for amyloid TTR, assuming a conservative 50% decrease in TTR degradation rates with amyloid deposition.

Acknowledging limitations, these results are preliminary and are only demonstrated within six individuals. As a result, we intend to perform further experiments to validate these findings.

Discussion

A Biophysical Model of Protein Homeostasis

Using these findings, we propose a biophysical model of protein homeostasis that explains how changes in PFS modify protein dynamics and amyloid formation. This model also identifies potential mechanisms by which age contributes to the amyloid cascade in ATTR. Our model enables the quantification of relative abundances of different structural proteoforms using quantified protein concentrations obtained using traditional proteomics and PFS values obtained using assays like IPSA (Figure 10).⁴²



B

$$K_{folding} = \frac{[P_m]}{[P_n]} \quad \Delta G_{folding} = -RT \ln(K_{folding}) \Rightarrow$$

$$[P_m] = [P_n] e^{-\frac{\Delta G}{RT}}, \quad [P_{total}] = [P_n] + [P_m] \Rightarrow$$

$$[P_{total}] = [P_n] + [P_n] e^{-\frac{\Delta G}{RT}} \Rightarrow$$

$$[P_n] = \frac{[P_{total}]}{1 + e^{-\frac{\Delta G}{RT}}}, \quad [P_m] = \frac{[P_{total}]}{1 + e^{-\frac{\Delta G}{RT}}} * e^{-\frac{\Delta G}{RT}}$$

Figure 10: Quantifying Folding States Using Protein Abundances and PFS. (A) The equilibrium between folded (P_n) and misfolded proteins (P_m) can be simplified using the assumption that unfolded proteins exist as a transient state and rapidly fold into properly folded or misfolded states. (B) Using this simplification, the standard change in free energy at equilibrium equation, and the equation for total protein concentrations, the formula for concentrations of properly folded and misfolded proteins can be derived. Calculating these concentrations then only requires quantifying the total concentration of a protein (P_{total}) using traditional quantitative proteomics and $\Delta G_{folding}$ which can be done using IPSA as $C_{1/2}$ values are proportional to ΔG .¹³

In this model, PFS is the average of an equilibrium between different structural proteoforms which are established in part due to different PFS-dependent degradation rates (Figure 11). This is because unfolding rate constants between misfolded and properly folded proteins are not the same as evidenced by increased thermodynamic stability of amyloids.⁴³

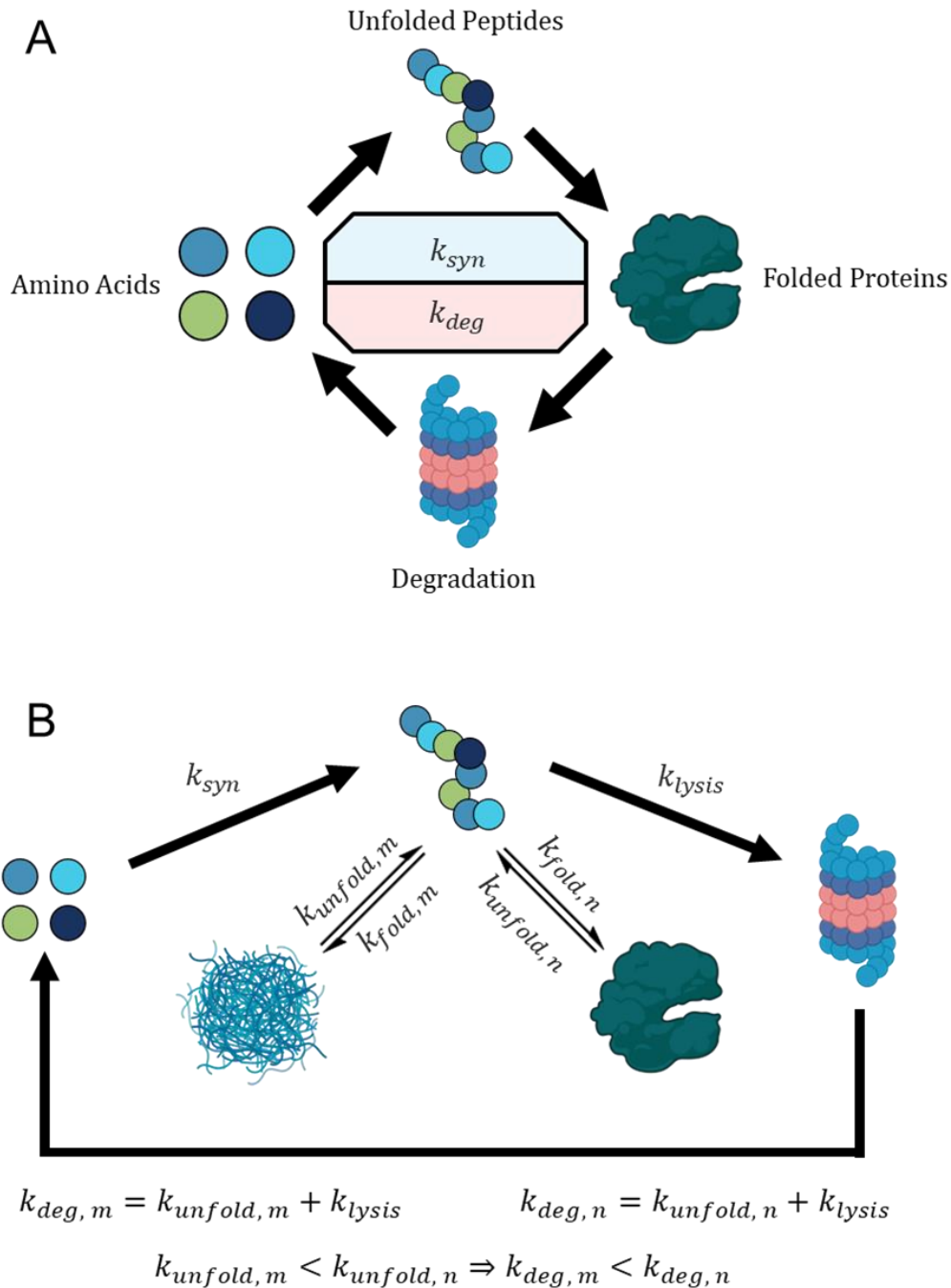


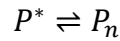
Figure 11: Protein Turnover Models. (A) The traditional model of protein turnover ignores protein folding, focusing on simplified rates of synthesis and degradation. (B) Factoring in protein folding and different protein folding states, the expanded model of protein turnover highlights different degradation rates for different structural proteoforms, consistent with our PFS-TR data. Unlike the traditional model, this model explains how amyloid deposits evade degradation.

Utilizing this model, as PFS of native proteins states decrease, allowing for more unfolding, relative concentrations of amyloid proteins increase, consistent with literature findings.⁴⁰ Considering that amyloid formation occurs through a process of nucleation and polymerization, this model is also able to account for differing rates of amyloid formation with age (Equation 1).

$$\frac{d[P_m]}{dt} = k_{fold,m}([P_m])[P^*] - k_{unfold,m}[P_m] \quad \text{(Equation 1)}$$

$$\frac{d[P_m]}{dt} = k_{fold,m}^*[P_m][P^*] - k_{unfold,m}[P_m]$$

$$[P_m] = c_1 \exp\left((k_{fold,m}^*[P^*] - k_{unfold,m})t\right)$$



Amyloid acts as a nucleation site and catalyst for new amyloid formation as indicated in Equation 2. Therefore in our model, the amyloid formation rate is dependent on the current concentration of amyloid (P_m) and the unfolded form of the protein (P^*),⁴⁴ we will denote the rate constant for misfolding as the function, $k_{fold,m}([P_m])$ where rate is dependent on amyloid concentrations, $[P_m]$. We can express the rate of amyloid formation as $k_{fold,m}^*[P_m][P^*]$ because initial velocities of enzymatic reactions increase proportionally to increases in enzyme concentration and $[P^*]$ remains at a small equilibrium value with fast protein folding kinetics.^{45,46} Factoring in $[P^*]$, this model is also able to explain observed trends of increased rates of aggregation at higher concentrations of aggregation-prone proteins as increases in protein concentrations impact equilibrium concentrations of folding intermediates.⁴⁷ As regulated degradation of aberrant proteins is also impaired with age,⁴⁸ $k_{unfold,m}$ decreases with age, meaning that

aging and amyloid formation are an aggressive positive feedback loop. Solving the first order ordinary differential equation presented, we find that amyloid concentrations inherently increase with age, matching existing literature.⁴⁹

A Biophysical Mechanism for ATTR Pathogenesis

Applying our model to ATTR with our results from our in-vivo census of PFS with age, we propose a novel mechanism for age-dependent ATTR pathogenesis (Figure 12).

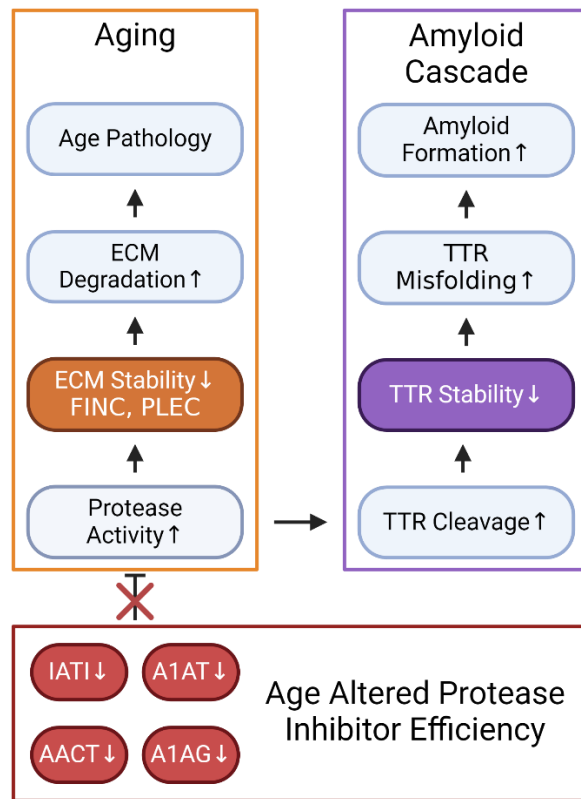


Figure 12: Age-dependent Pathogenesis of ATTR. Decreases in protease inhibitor efficiency with age promote protease activity as measured by changes in ECM stability. Increases in protease activity leads to increased proteolytic cleavage of TTR, promoting instability, misfolding, and amyloid formation.

Our results suggest that TTR amyloid formation is exaggerated by increased proteolytic activity due to age related decreases in SPI efficiency. The age-dependent

decrease in PFS of TTR along the dimer axis as opposed to the homodimer axis suggests that proteolytic cleavage introduces increased instability at the interface between monomers along the dimer axis. Hence, age does not appear to directly encourage kinetic dissociation along the homodimer axis. Instead, TTR cleavage into amyloidogenic fragments triggers the amyloid cascade by introducing nucleation sites. These nucleation sites can then interact with other TTR fragments or kinetically dissociated homodimers to form amyloid plaques. Increased stability of these amyloid plaques and impaired degradation pathways with age result in decreased degradation rates, preventing amyloid clearing. As a result, TTR deposition is progressive with age and leads to irreversible effects.

Increased proteolytic cleavage of ATTR with age potentially explains decreased effectiveness of kinetic stabilizer treatments at preventing amyloid formation in advanced-stage ATTR and after long-term treatment⁵⁰ as propensity of cleavage is independent of kinetic stabilization and can promote amyloid seeding, leading to increased rates of aggregation independent of tetramer dissociation rates. As a result, kinetic stabilizer treatments can only slow aggregation of dissociated tetramers but cannot prevent other sources of amyloid formation.

Conclusions

Imbalances in protein homeostasis associated with aging play a major role in the development of many currently untreatable diseases.⁵¹ Protein misfolding and formation of aggregates are hallmarks of many of these diseases such as ATTR and are inherent with aging,⁴⁹ but their causes and mechanisms are still not well understood due to limitations in traditional methodologies.⁴

In this study, we set out to identify how protein folding stability contributes to protein dynamics, aging pathology, and ATTR. We initiated the first-ever to our knowledge census of PFS on a proteomic scale in human serum from individuals across a wide range of ages and used IPSA to overcome limitations in previous studies by probing age-dependent changes in protein folding under physiological conditions. Additionally, we examined the role of PFS in protein homeostasis by directly comparing PFS and experimentally determined turnover rates.

We demonstrated that PFS plays an important role in TR and protein dynamics with important implications for amyloid formation and degradation. We have also identified a potential source of protease dysregulation with age due to structural differences in SPIs and have identified regions of TTR that display instability due to aging. Using these findings, we have proposed a model explaining the pathogenesis of age-dependent ATTR and a biophysical model of protein homeostasis that explains why amyloids form with age and are not degraded.

Regarding the limitations of these findings, our results displayed are preliminary. Our current sample size is twenty individuals for the PFS-age portion of the study and six individuals for the PFS-TR portion of the study. We have also largely sampled from individuals of European descent with connections to Brigham Young University. Furthermore, improvements can still be made to the resolution and coverage of PFS measurements in many of our samples. We also acknowledge that our findings do not explain why protease inhibitor efficiency decreases with age and that more targeted assays must be performed to explain the underlying mechanism.

Despite these limitations, our findings are compelling and tie together many observations from existing literature, warranting further investigation. As such, we aim to continue our PFS-age portion of the study, expanding our sample size to 150 individuals and aim to perform a larger-scale PFS-TR study within a mouse model. In the future, as our sampling limitations decrease, we aim to include samples from a more diverse population. We also intend to examine the role of mutations identified from our exome sequencing and other lifestyle factors collected in our sampling in PFS and ATTR.

In conclusion, our study provides novel insight into disruptions of protein homeostasis with age and introduces new insight into how ATTR and other aging pathologies can be remedied. Understanding which proteins experience pathogenic changes in stability with age allows for the development of targeted treatment methods to remedy folding-associated aging pathology and prevent the genesis of misfolding diseases. Our findings also highlight the benefits of introducing the dimension of PFS into the study of disease. Measuring changes in protein folding is essential to understanding the biophysical roots of many of today's most impactful diseases such as Alzheimer's and Parkinsons, and we have demonstrated that IPSA can be readily applied in human cohorts under physiological conditions to provide biologically significant insight into disease pathogenesis and pathophysiology. Hence, future application of IPSA within the context of other diseases is warranted, and we invite other researchers to introduce the essential dimension of PFS to their studies using IPSA and similar methods. Doing so will illuminate a more complete picture of protein homeostasis and will empower a greater understanding of human health, disease mechanisms, and drug and intervention development.

References

- (1) Díaz-Villanueva, J. F.; Díaz-Molina, R.; García-González, V. Protein Folding and Mechanisms of Proteostasis. *Int J Mol Sci* **2015**, *16* (8), 17193-17230. DOI: 10.3390/ijms160817193 From NLM.
- (2) Hipkiss, A. R. Accumulation of altered proteins and ageing: Causes and effects. *Experimental Gerontology* **2006**, *41* (5), 464-473. DOI: <https://doi.org/10.1016/j.exger.2006.03.004>.
- (3) Basaiawmoit, R. V.; Rattan, S. I. S. Cellular Stress and Protein Misfolding During Aging. In *Protein Misfolding and Cellular Stress in Disease and Aging: Concepts and Protocols*, Bross, P., Gregersen, N. Eds.; Humana Press, 2010; pp 107-117.
- (4) Grune, T.; Jung, T.; Merker, K.; Davies, K. J. A. Decreased proteolysis caused by protein aggregates, inclusion bodies, plaques, lipofuscin, ceroid, and 'aggresomes' during oxidative stress, aging, and disease. *The International Journal of Biochemistry & Cell Biology* **2004**, *36* (12), 2519-2530. DOI: <https://doi.org/10.1016/j.biocel.2004.04.020>.
- (5) Brailovsky, Y.; Rajapreyar, I.; Alvarez, R. TTR Amyloidosis: Current State of Affairs and Promise for the Future. *JACC Case Rep* **2023**, *10*, 101759. DOI: 10.1016/j.jaccas.2023.101759 From NLM.
- (6) Martyn, T.; Rubio, A. C.; Estep, J. D.; Hanna, M. Opportunities for Earlier Diagnosis and Treatment of Cardiac Amyloidosis. *Methodist Debaque Cardiovasc J* **2022**, *18* (5), 27-39. DOI: 10.14797/mdcvj.1163 From NLM.

- (7) Ruberg, F. L.; Grogan, M.; Hanna, M.; Kelly, J. W.; Maurer, M. S. Transthyretin Amyloid Cardiomyopathy: JACC State-of-the-Art Review. *J Am Coll Cardiol* **2019**, *73* (22), 2872-2891. DOI: 10.1016/j.jacc.2019.04.003 From NLM.
- (8) Bajwa, F.; O'Connor, R.; Ananthasubramaniam, K. Epidemiology and clinical manifestations of cardiac amyloidosis. *Heart Failure Reviews* **2022**, *27* (5), 1471-1484. DOI: 10.1007/s10741-021-10162-1.
- (9) Acquasaliente, L.; De Filippis, V. The Role of Proteolysis in Amyloidosis. *International Journal of Molecular Sciences* **2023**, *24* (1), 699.
- (10) Peterson, S. A.; Klabunde, T.; Lashuel, H. A.; Purkey, H.; Sacchettini, J. C.; Kelly, J. W. Inhibiting transthyretin conformational changes that lead to amyloid fibril formation. *Proceedings of the National Academy of Sciences* **1998**, *95* (22), 12956-12960. DOI: doi:10.1073/pnas.95.22.12956.
- (11) Jiang, X.; Buxbaum, J. N.; Kelly, J. W. The V122I cardiomyopathy variant of transthyretin increases the velocity of rate-limiting tetramer dissociation, resulting in accelerated amyloidosis. *Proceedings of the National Academy of Sciences* **2001**, *98* (26), 14943-14948. DOI: doi:10.1073/pnas.261419998.
- (12) Bezerra, F.; Niemietz, C.; Schmidt, H. H. J.; Zibert, A.; Guo, S.; Monia, B. P.; Gonçalves, P.; Saraiva, M. J.; Almeida, M. R. In Vitro and In Vivo Effects of SerpinA1 on the Modulation of Transthyretin Proteolysis. *Int J Mol Sci* **2021**, *22* (17). DOI: 10.3390/ijms22179488 From NLM.
- (13) Lin, H.-J. L.; James, I.; Hyer, C. D.; Haderlie, C. T.; Zackrisson, M. J.; Bateman, T. M.; Berg, M.; Park, J.-S.; Daley, S. A.; Zuniga Pina, N. R.; et al. Quantifying In Situ Structural Stabilities of Human Blood Plasma Proteins Using a Novel

- Iodination Protein Stability Assay. *Journal of Proteome Research* **2022**, *21* (12), 2920-2935. DOI: 10.1021/acs.jproteome.2c00323.
- (14) Naylor, B. C.; Porter, M. T.; Wilson, E.; Herring, A.; Lofthouse, S.; Hannemann, A.; Piccolo, S. R.; Rockwood, A. L.; Price, J. C. Deuterater: a tool for quantifying peptide isotope precision and kinetic proteomics. *Bioinformatics* **2017**, *33* (10), 1514-1520. DOI: 10.1093/bioinformatics/btx009 (accessed 4/30/2024).
- (15) Danecek, P.; Bonfield, J. K.; Liddle, J.; Marshall, J.; Ohan, V.; Pollard, M. O.; Whitwham, A.; Keane, T.; McCarthy, S. A.; Davies, R. M.; et al. Twelve years of SAMtools and BCFtools. *Gigascience* **2021**, *10* (2). DOI: 10.1093/gigascience/giab008 From NLM.
- (16) Cesnik, A. J.; Miller, R. M.; Ibrahim, K.; Lu, L.; Millikin, R. J.; Shortreed, M. R.; Frey, B. L.; Smith, L. M. Spritz: A Proteogenomic Database Engine. *J Proteome Res* **2021**, *20* (4), 1826-1834. DOI: 10.1021/acs.jproteome.0c00407 From NLM.
- (17) Burger, B.; Vaudel, M.; Barsnes, H. Importance of Block Randomization When Designing Proteomics Experiments. *Journal of Proteome Research* **2021**, *20* (1), 122-128. DOI: 10.1021/acs.jproteome.0c00536.
- (18) Hyer, C. D.; Lin, H.-J. L.; Haderlie, C. T.; Berg, M.; Price, J. C. CHalf: Folding Stability Made Simple. *Journal of Proteome Research* **2023**, *22* (2), 605-614. DOI: 10.1021/acs.jproteome.2c00619.
- (19) Jumper, J.; Evans, R.; Pritzel, A.; Green, T.; Figurnov, M.; Ronneberger, O.; Tunyasuvunakool, K.; Bates, R.; Žídek, A.; Potapenko, A.; et al. Highly accurate protein structure prediction with AlphaFold. *Nature* **2021**, *596* (7873), 583-589. DOI: 10.1038/s41586-021-03819-2.

- (20) Varadi, M.; Anyango, S.; Deshpande, M.; Nair, S.; Natassia, C.; Yordanova, G.; Yuan, D.; Stroe, O.; Wood, G.; Laydon, A.; et al. AlphaFold Protein Structure Database: massively expanding the structural coverage of protein-sequence space with high-accuracy models. *Nucleic Acids Research* **2021**, *50* (D1), D439-D444. DOI: 10.1093/nar/gkab1061 (accessed 5/3/2024).
- (21) Carrell, R. W.; Mushunje, A.; Zhou, A. Serpins show structural basis for oligomer toxicity and amyloid ubiquity. *FEBS Lett* **2008**, *582* (17), 2537-2541. DOI: 10.1016/j.febslet.2008.06.021 From NLM.
- (22) Dementiev, A.; Dobó, J.; Gettins, P. G. W. Active Site Distortion Is Sufficient for Proteinase Inhibition by Serpins: STRUCTURE OF THE COVALENT COMPLEX OF α 1-PROTEINASE INHIBITOR WITH PORCINE PANCREATIC ELASTASE*. *Journal of Biological Chemistry* **2006**, *281* (6), 3452-3457. DOI: <https://doi.org/10.1074/jbc.M510564200>.
- (23) Baumann, U.; Huber, R.; Bode, W.; Grosse, D.; Lesjak, M.; Laurell, C. B. Crystal structure of cleaved human α 1-antichymotrypsin at 2.7 Å resolution and its comparison with other serpins. *Journal of Molecular Biology* **1991**, *218* (3), 595-606. DOI: [https://doi.org/10.1016/0022-2836\(91\)90704-A](https://doi.org/10.1016/0022-2836(91)90704-A).
- (24) Lawrence, D. A.; Ginsburg, D.; Day, D. E.; Berkenpas, M. B.; Verhamme, I. M.; Kvassman, J.-O.; Shore, J. D. Serpin-Protease Complexes Are Trapped as Stable Acyl-Enzyme Intermediates (*). *Journal of Biological Chemistry* **1995**, *270* (43), 25309-25312. DOI: <https://doi.org/10.1074/jbc.270.43.25309>.

- (25) Teixeira, C.; Martins, H. S.; Saraiva, M. J. Cellular environment of TTR deposits in an animal model of ATTR—Cardiomyopathy. *Frontiers in Molecular Biosciences* **2023**, *10*, 1144049.
- (26) Sepúlveda, C.; Palomo, I.; Fuentes, E. Primary and secondary haemostasis changes related to aging. *Mechanisms of Ageing and Development* **2015**, *150*, 46-54. DOI: <https://doi.org/10.1016/j.mad.2015.08.006>.
- (27) Yaron, J. R.; Zhang, L.; Guo, Q.; Haydel, S. E.; Lucas, A. R. Fibrinolytic Serine Proteases, Therapeutic Serpins and Inflammation: Fire Dancers and Firestorms. *Front Cardiovasc Med* **2021**, *8*, 648947. DOI: 10.3389/fcvm.2021.648947 From NLM.
- (28) Antia, M.; Baneyx, G.; Kubow, K. E.; Vogel, V. Fibronectin in aging extracellular matrix fibrils is progressively unfolded by cells and elicits an enhanced rigidity response. *Faraday Discussions* **2008**, *139* (0), 229-249, 10.1039/B718714A. DOI: 10.1039/B718714A.
- (29) Oegema, T. R. J.; Johnson, S. L.; Aguiar, D. J.; Ogilvie, J. W. Fibronectin and Its Fragments Increase With Degeneration in the Human Intervertebral Disc. *Spine* **2000**, *25* (21), 2742-2747.
- (30) Wang, J.; Yin, L.; Chen, Z. New insights into the altered fibronectin matrix and extrasynaptic transmission in the aging brain. *Journal of Clinical Gerontology and Geriatrics* **2011**, *2* (2), 35-41. DOI: <https://doi.org/10.1016/j.jcgg.2010.12.002>.
- (31) Volpi, E.; Nazemi, R.; Fujita, S. Muscle tissue changes with aging. *Current Opinion in Clinical Nutrition & Metabolic Care* **2004**, *7* (4), 405-410. DOI: 10.1097/01.mco.0000134362.76653.b2.

- (32) Ubaida-Mohien, C.; Lyashkov, A.; Gonzalez-Freire, M.; Tharakan, R.; Shardell, M.; Moaddel, R.; Semba, R. D.; Chia, C. W.; Gorospe, M.; Sen, R.; et al. Discovery proteomics in aging human skeletal muscle finds change in spliceosome, immunity, proteostasis and mitochondria. *eLife* **2019**, *8*, e49874. DOI: 10.7554/eLife.49874.
- (33) Parthiban, G. P.; Wilson, J.; Nesheiwat, J. Amyloid Myopathy: A Cunning Masquerader. *Cureus* **2023**, *15* (5).
- (34) Andrä, K.; Nikolic, B.; Stöcher, M.; Drenckhahn, D.; Wiche, G. Not just scaffolding: plectin regulates actin dynamics in cultured cells. *Genes & development* **1998**, *12* (21), 3442-3451.
- (35) Saido, T.; Leissring, M. A. Proteolytic degradation of amyloid β -protein. *Cold Spring Harb Perspect Med* **2012**, *2* (6), a006379. DOI: 10.1101/cshperspect.a006379 From NLM.
- (36) Toyama, B. H.; Weissman, J. S. Amyloid structure: conformational diversity and consequences. *Annu Rev Biochem* **2011**, *80*, 557-585. DOI: 10.1146/annurev-biochem-090908-120656 From NLM.
- (37) Li, F.; Leier, A.; Liu, Q.; Wang, Y.; Xiang, D.; Akutsu, T.; Webb, G. I.; Smith, A. I.; Marquez-Lago, T.; Li, J. Procleave: predicting protease-specific substrate cleavage sites by combining sequence and structural information. *Genomics, Proteomics and Bioinformatics* **2020**, *18* (1), 52-64.
- (38) Yang, Y.; Guo, R.; Gaffney, K.; Kim, M.; Muhammednazaar, S.; Tian, W.; Wang, B.; Liang, J.; Hong, H. Folding-Degradation Relationship of a Membrane Protein Mediated by the Universally Conserved ATP-Dependent Protease FtsH. *Journal of*

- the American Chemical Society* **2018**, *140* (13), 4656-4665. DOI: 10.1021/jacs.8b00832.
- (39) De Baets, G.; Reumers, J.; Delgado Blanco, J.; Dopazo, J.; Schymkowitz, J.; Rousseau, F. An evolutionary trade-off between protein turnover rate and protein aggregation favors a higher aggregation propensity in fast degrading proteins. *PLoS Comput Biol* **2011**, *7* (6), e1002090. DOI: 10.1371/journal.pcbi.1002090 From NLM.
- (40) Espargaró, A.; Castillo, V.; de Groot, N. S.; Ventura, S. The in Vivo and in Vitro Aggregation Properties of Globular Proteins Correlate With Their Conformational Stability: The SH3 Case. *Journal of Molecular Biology* **2008**, *378* (5), 1116-1131. DOI: <https://doi.org/10.1016/j.jmb.2008.03.020>.
- (41) Schwanhäusser, B.; Busse, D.; Li, N.; Dittmar, G.; Schuchhardt, J.; Wolf, J.; Chen, W.; Selbach, M. Global quantification of mammalian gene expression control. *Nature* **2011**, *473* (7347), 337-342. DOI: 10.1038/nature10098.
- (42) Lin, H.-J. L. Quantifying Protein Quality to Understand Protein Homeostasis. Doctoral Dissertation, Brigham Young University, Provo, UT, 2022. <https://scholarsarchive.byu.edu/etd/9618>.
- (43) Willbold, D.; Strodel, B.; Schröder, G. F.; Hoyer, W.; Heise, H. Amyloid-type Protein Aggregation and Prion-like Properties of Amyloids. *Chemical Reviews* **2021**, *121* (13), 8285-8307. DOI: 10.1021/acs.chemrev.1c00196.
- (44) Chatani, E.; Yamamoto, N. Recent progress on understanding the mechanisms of amyloid nucleation. *Biophys Rev* **2018**, *10* (2), 527-534. DOI: 10.1007/s12551-017-0353-8 From NLM.

- (45) Robinson, P. K. Enzymes: principles and biotechnological applications. *Essays Biochem* **2015**, *59*, 1-41. DOI: 10.1042/bse0590001 From NLM.
- (46) Schonbrun, J.; Dill, K. A. Fast protein folding kinetics. *Proceedings of the National Academy of Sciences* **2003**, *100* (22), 12678-12682. DOI: doi:10.1073/pnas.1735417100.
- (47) Ajmal, M. R. Protein Misfolding and Aggregation in Proteinopathies: Causes, Mechanism and Cellular Response. *Diseases* **2023**, *11* (1). DOI: 10.3390/diseases11010030 From NLM.
- (48) Vernace, V. A.; Schmidt-Glenewinkel, T.; Figueiredo-Pereira, M. E. Aging and regulated protein degradation: who has the UPPER hand? *Aging Cell* **2007**, *6* (5), 599-606. DOI: 10.1111/j.1474-9726.2007.00329.x From NLM.
- (49) David, D. C.; Ollikainen, N.; Trinidad, J. C.; Cary, M. P.; Burlingame, A. L.; Kenyon, C. Widespread Protein Aggregation as an Inherent Part of Aging in *C. elegans*. *PLOS Biology* **2010**, *8* (8), e1000450. DOI: 10.1371/journal.pbio.1000450.
- (50) Morfino, P.; Aimo, A.; Vergaro, G.; Sanguinetti, C.; Castiglione, V.; Franzini, M.; Perrone, M. A.; Emdin, M. Transthyretin Stabilizers and Seeding Inhibitors as Therapies for Amyloid Transthyretin Cardiomyopathy. *Pharmaceutics* **2023**, *15* (4). DOI: 10.3390/pharmaceutics15041129 From NLM.
- (51) Hipp, M. S.; Kasturi, P.; Hartl, F. U. The proteostasis network and its decline in ageing. *Nature Reviews Molecular Cell Biology* **2019**, *20* (7), 421-435. DOI: 10.1038/s41580-019-0101-y.

Some figures created using BioRender.com

Molecular graphics and analyses performed with UCSF Chimera, developed by the Resource for Biocomputing, Visualization, and Informatics at the University of California, San Francisco, with support from NIH P41-GM103311.